Title

Unbiased Quantification of Subplate Neuron Loss following Neonatal Hypoxia-Ischemia in a Rat Model

Authors

Mikhailova, Alexandra
Sunkara, Naveena
McQuillen, Patrick S

Unbiased Quantification of Subplate Neuron Loss Following Neonatal Hypoxia Ischemia in a Rat Model

Alexandra Mikhailova, **Naveena Sunkara**, and **Patrick S. McQuillen**

Department of Pediatrics, School of Medicine, University of California San Francisco

Abstract

Background—Cellular targets of neonatal hypoxia ischemia (HI) include both oligodendrocyte and neuronal lineages with differences in the patterns of vulnerable cells depending upon the developmental stage at which the injury occurs. Injury to the developing white matter is a characteristic feature of human preterm brain injury. Data is accumulating however for neuronal injury in the developing cerebral cortex. In the most widely used rodent model of preterm HI brain injury, conflicting data has been reported regarding the sensitivity of subplate neurons to early neonatal HI, with some reports of selective vulnerability while others find no increased loss of subplate neurons in comparison with other cortical layers. Methods used to identify subplate neurons and quantify their numbers vary among studies.

Objective—To use recently developed cortical layer specific markers quantified with definitive stereologic methods to determine magnitude and specificity of subplate neuron cell loss following neonatal HI in a rodent model.

Methods—Postnatal day two (P2) rats underwent right common carotid artery coagulation followed by 2–3 hours of hypoxia (5.6% oxygen). Categorically moderately injured brains were stained with subplate and cortical layer III – V markers (Complexin3 and Foxp1, respectively) at P8 and P21 (Foxp1 only). Optical Fractionator was used to quantify subplate and middle/lower cortical neuronal number and compared across groups (naive control, hypoxia hemisphere and hypoxia-ischemia hemisphere).

Results—Following HI at P2 in rat, total Complexin3-expressing subplate neuron number decreases significantly in the HI hemisphere compared with naïve controls or hypoxia alone (HI vs. control mean+/−SD, 26747+/−7952 vs. 35468+/−8029, P = 0.04; HI vs. hypoxia, 26747+/−7952 vs. 40439+/−7363, P=0.003). In contrast, total Foxp1-expressing layer III–V cell number is not different across the three conditions at P8 (HI vs. control mean+/−SD, 1195085+/−436609 vs. 1234640+/−178540, P = 0.19; HI vs. hypoxia, 1195085+/−436609 vs. 1289195+/−468941, P=0.35) and at P21 (HI vs. control mean+/−SD, 1265190+/−48089 vs. 1195632 +/−26912, P = 0.19; HI vs. hypoxia, 1265190+/−48089 vs. 1309563+/−41669, P=0.49).

Conclusions—There is significant biological variability inherent in both subplate neuron cell number and the pattern and severity of cortical injury following HI at P2 in rat. Despite this variability, subplate neuron cell number is lower following P2 HI in animals with mild or moderate

Corresponding Author Address: Patrick S McQuillen, Arthur and Toni Rembe Rock Hall Mission Bay, University of California, San Francisco, 1550 4th Street rm RH-384E, San Francisco CA 94158-2711, United States, Phone: 415-502-4798, Fax: 415-502-2374.

cortical injury while middle to lower layer cortical neuronal number is unchanged. In more severe cases, neurons are lost from lower cortical layers suggesting a relative vulnerability of subplate neurons.

Keywords

optical fractionator; cortical layer specific marker; brain injury; premature newborn

Introduction

Brain injury associated with premature birth is a major and increasing worldwide problem resulting in lifelong disability with substantial social and economic burdens [1,2]. The incidence of premature birth is rising along with improved survival even at extreme limits of viability. Rates of cognitive and behavioral disabilities rise with decreasing gestational age at birth [3]. Together these trends result in a growing population of children with substantial neurodevelopmental disability.

Neurobiological substrates of motor disabilities following neonatal brain injury (e.g. cerebral palsy) have been attributed to specific neuroanatomical injuries. Spastic diplegia, for example, is thought to result from injury to myelinated pyramidal tract motor axons as they pass close by margins of the lateral ventricles coinciding with the common location for cystic white matter injury (periventricular leukomalacia) [4]. The neurobiological substrates for cognitive and behavioral impairments are not as well understood but are likely to emerge from more widespread injuries involving multiple cortical areas.

Animal models that faithfully reproduce brain injuries in human preterm infants are needed to gain insight into cellular and developmental mechanisms resulting in dysfunction of neural systems. Hypoxia ischemia (HI) and inflammation are the most frequent causes of neonatal brain injury and result in lifelong motor and cognitive disability [5]. Thus HI, with or without additional inflammation, in rodents is the most common model of neonatal brain injury. Using this model immediately after birth combined with birthdating methods, we reported selective vulnerability of subplate neurons following HI at P2 [6]. The injury was deemed selective based upon a decrease in subplate neurons even in mild injuries, where no histologic injury could be noted in nissl stained cortex. Severely injured cases were noted to have loss of lower layer neurons [6,7].

This report was among the first to note direct neuronal injury following neonatal HI in additional to more widely studied injury to preoligodendrocytes [8] and activation of astrocytes [9] and microglia [10]. Subplate neurons play critical roles at many stages of cortical development before undergoing programmed cell death [11–13]. Subplate neurons pioneer projections from cortex to thalamus and in turn receive the first thalamic inputs [14–16]. Subplate neurons send a projection into layer IV of neocortex and thus form a transient developmental circuit through which they influence early cortical activity [17]. Subplate neurons play a role in the maturation of both excitatory and inhibitory cortical synapses [7,18,19]. Premature removal of subplate neurons alters specific cortical activity patterns and reduces the capacity for both early somatosensory barrel plasticity and later ocular dominance plasticity [7,20–22]. Thus, involvement of subplate neurons in a model of early

brain injury offered a potential mechanism for widespread dysfunction of cortical circuits observed following very preterm human birth.

Until recently, subplate neurons were identified by their characteristic morphology (inverted pyramidal), location at the base of neocortex (e.g. layer VIb in rat) and by their early birthdates [23]. However, as with neurons in all neocortical layers, subplate neurons are a pleomorphic population. Even prior to the development of cortical layer specific markers, it was known that subplate neurons consisted of both excitatory and inhibitory populations with differing projection patterns [17]. With the advent of large-scale projects to survey regional and developmental gene expression (e.g. Allen Institute Brain Atlas Project), new markers were described for most cortical layers, including subplate [24]. Using these and other markers, further diversity has been demonstrated for neurons in the subplate layer [25].

Given the conceptual importance of subplate neuron injury for neurodevelopmental impairments following human preterm birth and to more fully characterize the specific vulnerability of subplate neurons in this model, we used cortical layer specific markers and definitive stereological methods to quantify subplate neuron number following neonatal HI.

Materials and Methods

Animals

Timed-pregnant Long Evans rats of both genders (Simonsen) were allowed food and water *ad libitum*. All animal research was approved by the University of California San Francisco Committee on Animal Research and was performed in accordance with standards of humane care set forth in the *Policy on Humane Care and Use of Laboratory Animals*.

Hypoxia-ischemia

Procedure described previously [7,22]. The manipulation was performed at postnatal day P2 (day of birth = P0). To produce ischemia, pups were individually anesthetized with isoflurane. A midline incision was made in the neck; the right common carotid artery was dissected from the jugular vein and coagulated with a bipolar coagulator. Animals were returned to the dam for 1–2 hr. to recover from anesthesia and feed. Subsequently, pups receiving hypoxia were placed in 5.6% oxygen in temperature controlled chambers maintained between 34–35°C for 2–3 hrs. One pup from each litter was monitored with a skin surface temperature probe and the chamber temperature adjusted to keep skin temperature (35.5–37°C). Hypoxia was continued for a maximum of 3.5 hours or terminated for any individual pup at any signs of agonal respirations or any persistent clonic or tonic-clonic movements. At postnatal day 8 or 21, rat pups were sacrificed with pentobarbital, 100 mg/kg, given by intraperitoneal injection.

Immunohistochemistry

Animals were perfused transcardially with 0.1 M phosphate buffer followed by cold 4% paraformaldehyde in 0.1 M phosphate buffer. Perfused brains were postfixed for 6 hrs. and then cryoprotected in 25% sucrose in 0.1 M phosphate buffer overnight prior to sectioning on a sliding microtome. Eighty micrometer sections were quenched with 3% hydrogen

peroxide, washed, and blocked (5% donkey serum, 10% BSA, 5% fish skin gelatin, and 0.1% Triton X-100 in 0.1 M phosphate-buffered saline). Primary antibody dilutions used were 1:5,000 for anti-Complexin3 (rabbit polyclonal, 122 302; Synaptic Systems) and 1:50,000 for anti-Foxp1 (mouse monoclonal, ab32010; AbCam). Primary antibody was applied overnight at 4°C. Secondary antibody 1:500, (biotinylated donkey anti-mouse or biotinylated donkey anti-rabbit; Jackson ImmunoResearch) was applied for 1 hr. at room temperature. The sections were washed and incubated with avidin-biotinylated complex (ABC) using the Vectastain Elite kit (Vector Laboratories, Burlingame, CA) for 2 hours. Lastly, the sections were washed and developed in a solution of 3,3′-diaminobenzidine (Sigma, St. Louis, MO) and nickel sulfate for 3 minutes. For fluorescent labeling, the same procedure was followed, omitting hydrogen peroxide incubation. Following primary incubation and washing, sections were incubated with secondary antibodies 1:500 donkey anti-rabbit (AlexaFluor488; Jackson) or 1:500 donkey anti-goat (AlexaFluor594; Life Technologies).

Quantification of cell numbers

We performed a formal stereology study that followed a systematic random sampling (SRS) scheme: sections were selected systematically (every 12th) from front to back of brain and the probing of sections was randomized such that all parts of the region of interest had an equal probability of being sampled. The subplate zone was identified as described previously [6] by cytoarchitectonic features of neocortex [23]. In the radial domain, the subplate (layer VIB) was localized at the base of the cortical plate, immediately below layer VI neurons, and contained characteristic inverted pyramidal neurons. The borders in the coronal domain extended to cingulate cortex in the medial direction and entorhinal cortex laterally. The rostral and caudal boundaries were determined empirically to allow for at least one section at each end of the brain to be discarded. Rostrally, the first sections were omitted if no corpus callosum present. Caudally, sections without cingulate cortex were omitted. The layers (III–V) were determined radially with Foxp1 heavily stained cells in the characteristic six-layered neocortex, with borders extending into cingulate cortex in the medial direction and entorhinal cortex laterally. The same rostral/caudal boundaries were used for subplate and cortical layer markers. Cell populations were estimated using the Optical Fractionator probe [26] in Stereo Investigator (MBF Bioscience, Williston, VT). We have reported the estimated population (number weighted section thickness) for all cell counts. Parameters for the Optical Fractionator study are given in Table 1. 4–6 sections were analyzed per animal at P8, 7–8 sections at P21. Individual cells were counted using standard stereological methods with a 63x oil immersion lens on a Zeiss Axioscope II epifluorescent microscope. Adequate sampling was verified with coefficients of error (Gundersen, m=1) below 0.1, and later analyzed for biological and stereological variability (see *Results*).

Statistics

Data was examined graphically with scatter plots to evaluate distribution and summarized as mean +/− SD. Sample population difference testing was performed with unpaired, two-sided Student's t-test. Association was tested by linear regression. Power calculations were performed using sample size, effect size and standard deviation as described [27]. Biological

variability was estimated using coefficient of variance (CV = SD/Mean) and coefficient of error (CE, as described [28]).

Results

Determining a markers for stereology

For a marker to be compatible with stereological counting procedures, it must localize to a discernible point or profile to determine that it falls within the boundaries of the counting frame/dissector. To select a subplate marker suitable for stereological counting, we examined 3 options previously used [25,29]: Complexin3, Nurr1 and CTGF. We performed fluorescent stains with Complexin3/Nurr1 and Complexin3/CTGF (Fig. 1). The three markers label overlapping but not identical subplate populations. Complexin3 may co-label with the Nurr1 or CTGF, but single positive cells for each marker are noted as well. Nurr1 staining is nuclear and technically ideal for counting (Fig. 1A′). However, Nurr1 labeled cortical cells outside of subplate, especially near entorhinal cortex. CTGF staining is cytoplasmic and punctate with irregular profiles and not ideal for top-counting (Fig. 1B′). Complexin3 is cytoplasmic, outlining the cell nucleus and, importantly, was the most robust with peroxidase-DAB staining, labeling cells only the subplate and not elsewhere in the cortex (Fig. 3A).

To select layer specific markers suitable for stereological quantification of cortical layers, we considered: Er81 (layer V), Tbr1 (layer VI), Foxp2 (layer VI), Ctip2 (layer V–VI) and Foxp1 (layers III–V). Er81 selectively labels a subpopulation of layer 5 cells, and some layer 3–4 (Yamamoto 2006). While Er81 worked robustly for Okusa et al [29], in our experience, a commercially available Er81 antibody (sc-28681, Santa Cruz Biotech) was not layer specific. Foxp1 was chosen because of its clean nuclear stain with clear layer specificity that included layer V.

Histological analysis of moderate HI injury at P8

The Vannucci procedure [30], unilateral CCL followed by bilateral hypoxia, produces a range of injury from mild to severe dependent upon a variety of factors including age, animal strain and temperature [31]. At P2, we have arbitrarily defined injury categories from mild (minimal to no histologic changes in neocortex and mild or no asymmetry of lateral ventricles in coronal plane), moderate (clear asymmetry of lateral ventricles with thinning or patchy dropout of layer VIb/subplate) and severe (widespread loss of layer VIb/subplate and/or laminar or columnar loss of cells in layer VIa) [7]. Severe cases often have cyst formation laterally with more extensive loss of cortical layers. Other investigators have reported similar patterns, although categorical definitions vary [32–34]. For continuous measures of injury severity, we have employed cortical thickness measured from the pial to ventricular surface over primary visual cortex adjacent to dentate gyrus at P30 [7]. More recently, we have measured infarct volumes with the Cavalieri method [22]. Eight litters (4 in early cohort, 4 in late cohort) were used for the present experiments. N=85 total pups, both genders were used, 12 of which were naive littermate controls. In total, 72 pups received HI at P2, with a procedural mortality of 12 (16%). Cortical injury was identified on coronal sections stained with Cresyl violet, and categorized based on above criteria. Out of

60 of animals surviving HI, 43 developed mild injury, 15 had moderate injury and 2 had severe injury. Histological changes including hemispheric asymmetry in the coronal plane and thinning of layer VIb following HI are shown in Fig. 2. At P8, hemispheric volumes ranged from 148–183 mm^3 in the hypoxia alone hemispheres and 124 – 183 mm^3 in HI exposed hemispheres. Infarct volumes (hypoxia hemisphere - HI hemisphere)/hypoxia hemisphere x 100) ranged from −2 to 15%. At P21, hemispheric volumes ranged from 220–324 mm^3 in the hypoxia alone hemispheres and 217–315 mm^3 in HI exposed hemispheres. Infarct volumes ranged from 0 to 13%.

Significant reduction in subplate cell population in HI injury group

Sections were selected using systematic random sampling and the Optical Fractionator method was used to quantify cell number [26]. For this procedure, contours were drawn using clear anatomical boundaries and guided by layer specific marker immunohistochemistry (boundaries summarized in Methods). Counting and sampling grid dimensions were determined with pilot studies (summarized in Table 1). Low magnification examples of the boundaries for both Complexin3 and Foxp1 are shown in Fig. 3A, 3B. Individual cells were counted following standard Stereological procedures and examples of counted cells are shown in Fig. 3C, 3D.

The total number of Complexin3-expressing cells was counted in the hypoxia and HI hemispheres of pups (N=8) with moderate brain injury and compared to naive controls (N=5). Hemispheric counts are summarized in Fig. 4A. Naive control animals have 35,456+/−8029 (mean+/−SD) cells per hemisphere at P8. Hemispheres exposed to hypoxia alone have 40,439+/−7363 cells per hemisphere. We found a significant decrease in cell number in the HI group, 26,747+/−7952 compared to hypoxia and naive control hemispheres (p=0.003 and p=0.004, respectively). Hemispheric ratios (right/left hemisphere) are presented to account for inter-animal variability in Complexin3 and Foxp1 cell numbers (Fig. 4C).

HI injury does not significantly reduce the number of cells in cortical layers III–IV at P8 or P21

To assess whether cell populations in middle to lower cortical layers were affected by hypoxic-ischemic insult at P8, we counted the number of Foxp1+ cells in in ipsi- and contralateral hemispheres of moderately injured hypoxic-ischemic brains (N=8) and compared to naive controls (N=5) (Fig. 4B). We found no significant changes in layer III–IV cell populations across the three injury groups. The average+/−SD number of Foxp1+ cells counted in control hemisphere is 1,234,640 +/−178,540 vs. HI hemisphere 1,195,085+/−436,609 (p=0.7).

To examine for late decreases in lower layer populations, we also quantified Foxp1+ cells in ipsi- and contralateral hemispheres of moderately injured hypoxic-ischemic brains (N=7) and compared to naive controls (N=8) at P21. Foxp1+ cell numbers are not significantly different between injury groups (Fig. 5A). The average +/−SD number of Foxp1+ cells counted in control hemispheres is 1,195,632 +/−26,912 vs. HI hemisphere 1,265,190+/−48,089 (P = 0.19). Hemispheric ratios (right/left) of Foxp1 counts have low variability between control and hypoxia (Fig. 5B). Foxp1 counts are not different when performed at P8

compared with P21 despite a 50% increase in brain size. HI hemisphere counts at P8 vs P21: 1,195,085 ± 67,544 vs. 1,265,190 ± 48,089 (P= 0.42). Control hemisphere counts at P8 vs P21: 1,234,640 ± 56,459 vs 1,195,632 +/−26,912 (P= 0.49).

We performed a power analysis to determine the chance of a Type II error for the Foxp1+ cortical neuron counts at P8. Using standard deviation from the control sample, the present sample size has a 92% power to detect a similar effect size (25% decrease) to that seen in Complexin3+ subplate neurons.

Subplate cell reduction and infarct volumes

Using birthdating techniques to identify subplate neurons, we find reduced subplate numbers even in mild injury categories [6]. Four HI treated animals in the present sample had no change in interhemispheric volume (Fig. 4D), despite a moderate histological grade of injury. Given the arbitrary nature of categorical injury scoring, we sought to determine if subplate neuron loss is predicted by injury measured by infarct volume. Infarct volumes are closely correlated with total HI Complexin3+ subplate cell number (Fig. 4D, $r^2 = 0.82$, p=0.0017) at P8, but not Foxp1+ cell number (Fig. 5C, r^2=0.56, p=0.14) at P21.

Biological vs. Stereological Variability in Subplate Neuron Cell Number

Complexin3-expressing subplate neuron counts demonstrate considerable variability (Fig. 4A, coefficient of variation, mean/S.D. = 22% control Complexin3). To evaluate the sources of variability in our study, we calculate the biological variability in comparison with stereological variability attributable to our sampling. Observed variance of the group (OCV^2_{GROUP}) is made up of true biological variance ($CV^2_{BIOLOGICAL}$) and stereological noise ($OCE^2_{(individual)}$) [28]. Biological variance cannot be directly calculated, but we can calculate observed variance ($SD^2/Mean^2$) and stereological noise (average of CE's, squared). We used the Gundersen coefficient of error (CE), with m=1, because the data is not 'smooth' - i.e. there is an inherent difference in distribution of cell numbers from front to back of brain. While the HI group had twice as much observed variance as control (0.088 vs. 0.046) both were made up of mostly biological variability (89% and 88%, respectively). These values indicate that stereological parameters were optimized for the population sampled, and variability in cell population estimates can be traced back to biological variability and not sampling errors.

Discussion

We have used modern cortical layer specific markers and definitive counting methods to evaluate subplate neuron loss in comparison to middle/lower cortical layer neuron loss following early hypoxia ischemia in a rodent model. We find significant loss of subplate, but not middle/lower layer cortical neurons in animals with a moderate degree of brain injury. Moreover, when we examine hemispheric infarct volume as a continuous measurement of brain injury severity, we see a linear relationship between infarct volume and subplate neuron number.

Okusa et al examined a similar model but were unable to confirm specific vulnerability of subplate neurons [29]. As with most reports using this model, they observed significant

variability in brain injury severity following HI at P2. Although, they report only finding strong effects on subplate neurons in severe cases, images of individual cases labeled with subplate specific markers show clear reduction in moderate cases. A number of factors may have contributed to these different conclusions including experimental and quantification methods, variability inherent in the model and evaluation of injury severity. Regarding the quantification methods, the Okusa study is notable for a large sample size (N=35) and blinding during quantification. However, the methods include a number of potential sources of bias. First subplate neuron cell density ratios are analyzed, rather than cell number and the individual sample sizes for each injury category are not reported, precluding any consideration of group variability and sample size. Second, sampling within each brain is limited to a single rostral caudal level and two sections. Third, no methods are presented for how individual cells were imaged or counted precluding any assessment of common sources of bias in counting studies. This is especially important with regards to some of the markers quantified including CTGF, which we contend is not suitable for precise cell counting owing to marker staining characteristics (i.e. diffuse and irregular profiles). The authors remark on considerable variability in their study and that the standard error of the means for percent cell reduction exceed percent differences many fold for all markers and injury category less than severe. However, they estimate a 14% (non-significant) decrease in Complexin3-expressing subplate neuron cell density in moderate cases. This effect size is comparable to our results where we note 24–34% reduction between hypoxia and HI hemispheres in moderate cases.

Several factors relating to methods and inherent variability in the Vannucci model should be considered. First, strain dependent variability has been well documented in mice [35] and likely exists in rat. Sprague Dawley rats are used in the study by Okusa et al, while we have used Long Evans rats exclusively [7,22] since an initial publication [6]. This choice is driven by a need to avoid albino strains for studies in visual system. Sizonenko and colleagues have reported results using Wistar strain [32,33,36]. Differences in the sensitivity of the strains can be noted by differences in the hypoxia dose and duration needed to produce injury: Long Evans (5.6% oxygen for 2–3 hours [7,22]), Sprague Dawley (6% oxygen for 2 hours [29]) and Wistar (6% oxygen for 30 minutes [32]). Temperature is also critically important. We maintain our chambers between 34–35°C and monitor skin surface temperature keeping a target temperature of 35.5–37°C. In the studies by Okusa et al and Sizonenko, chamber temperatures were set to 37°C. Despite these differences, comparable injury patterns are produced by all the groups (i.e. injury predominantly in the lower layers, cyst formation laterally in more severe cases). What is likely to vary is the distribution of injury, both across strains and with higher temperatures. Despite controlling all these factors, we find considerable variability in the distribution of mild, moderate and severe injuries across litters. A final methodologic difference relates to the technique of carotid ligation. Okusa et al ligate and divide the carotid artery, resulting in permanent loss of blood flow. We and others electrocoagulate the carotid artery. A method that produces reversible ischemia with recannulation of blood flow [37]. Variability of injury severity is a hallmark of hypoxic ischemic brain injury in human newborns.

Variable distribution of injury makes assessment of severity critical for comparing results across studies. We have reported the histological criteria for our categorical injury grade in

great detail and have correlated these histological patterns with diffusion weighted MRI at 24 hours post injury [7]. In practice however, histological patterns may vary enough that a categorical injury grade is an artificial construct that is difficult to reproduce across studies and groups. For example, Brockman et al have reported very similar histological patterns and MRI findings to our results although they include cases in their moderate group that we would grade as severe [34]. Further, in the present study, although we selected eight animals with moderate injury by histology, four of these had no measurable difference in hemispheric volume, suggesting a milder injury. Of these four animals, three showed substantial reductions of subplate neuron number. In addition to infarct volume, we have analyzed cortical thickness as a continuous measure of injury [7]. Cortical thickness predicts alterations in ocular dominance plasticity and differences in inhibitory neuron density as well as injury category [7]. However, cortical thickness is extremely dependent upon age and anatomical region. Hemispheric volumes are reliable and reproducible in this model when measured using accepted stereological methods (i.e. Cavalieri) [22]. Calculation of infarct volumes (contra - ipsi/contra) partially mitigates variability due to brain growth over time in immature rodent models. Considering all these factors, we conclude that infarct volume is the most reliable and unbiased method for measuring injury severity.

In addition to variability in the Vannucci model itself, we find substantial biological variability in hemispheric subplate neuron number (CV = 22%). This variability could have arisen from true biologic variability or to stereological noise. A distinct advantage of the Optical Fractionator method is that it allows for partition of relative sources variability. Consistent with our low coefficients of error, we find that more than 80% of the variability in subplate neuron number comes from true biologic variability. In other words, our results would not have been improved substantially by sampling more sections or sites [28]. With the Vannucci procedure, it is common to use the hypoxia alone hemisphere as a comparison to the HI hemisphere to reduce overall experimental variability and this was done in the study by Okusa et al. In the present study, doing so weakened the relationship between infarct volume and subplate neuron number. While hypoxia exposure alone does not result in overt histological injury or cell death, the treatment does lead to a variety of perturbations at the cellular and signaling level (e.g. stabilization of HIF1a and HIF signaling).

To the best of our knowledge, this is the first stereological study of subplate neuron number using layer specific markers. However, Robinson et al reported results quantifying ethidium bromide stained subplate neuron cell number, purportedly using stereological methods [38]. Their estimates of total subplate neuron number markedly exceed ours. However, these results must be taken with caution as their methods described in separate locations as either Optical Dissector or Physical Dissector, were actually an amalgamation of the latter with elements of $N_v * V_{ref}$ but missing adequate systematic random sampling. They perform top counting by comparing two confocal image planes, but only sample a 1 mm linear region. Furthermore, counts were performed by an automated software program and not using a standard stereological counting frame and rules. No specific markers are used for subplate neurons and they purport to distinguish between neurons and glia based on ethidium stained nuclear size. Finally, they estimate subplate layer volume simply by measuring brain anterior-posterior and medial-lateral dimensions and assume an oval shape. While their

estimates of subplate neuron number at P10 exceed ours at P8 by five or more fold, differences in the methods preclude direct comparison.

The present study has a number of important limitations. First, the subplate layer is heterogeneous, with multiple subpopulations [25]. By quantifying Complexin3, we are likely only capturing ~50% of all subplate neurons [25]. Furthermore, by quantifying subplate neuron cell number at P8, we underestimate subplate neuron cell loss because of substantial naturally occurring subplate programmed cell death, that peaks during the first postnatal week in rat [39]. We chose this age to enable direct comparison to the study by Okusa et al [29]. This age also allowed for sufficient time after injury for resolution of cell death and early edema. A second major issue is that we compare subplate neuron numbers to a marker, Foxp1, that identifies cell in layers III–V [40,41]. Ideally, we would have chosen to quantify a layer VI and layer V specific marker separately. However, commercially available antibodies for these markers either did not produce selective staining or were not compatible with stereological counting. By repeating the Foxp1 counts at P21, we have ruled out slow or delayed cortical neuronal death.

Why should subplate neurons manifest selective vulnerability? We have considered this issue in studies of immunopurified subplate neuron gene expression and response to excitotoxicity and find reduced expression of the GluR2 AMPA receptor and increased expression of metabotropic glutamate receptor 3 [42], both of which could account for an intrinsic cellular sensitivity to glutamate excitotoxicity. An additional hypothesis relates to the early generation and maturation of subplate neurons during cortical development [43]. Subplate neurons are among the first cortical neurons generated. They become morphologically mature before other cortical neurons, receive functional inputs and are integrated into transient cortical circuits before other cortical neurons [11,44]. In the process, subplate neurons are exposed to sources of potential excitotoxicity before other cortical layers. This rationale may explain the relative resistance of middle to upper layer neurons, especially layer II/III in which horizontal connections are known to develop relatively late [45]. Lower cortical layers are predominantly output layers, with descending, callosal and inter-areal projections. However, lower cortical layers make and receive excitatory inputs from subplate and thalamus [46]. Thus, the early sensitivity of subplate neurons may be a developmental phenomenon and only relative, especially as cortical circuits mature. Lower layer neurons are also involved with more severe injuries. That being said, subplate neuron injury has substantial impact on early cortical activity, activity dependent neuronal maturation of both excitatory and inhibitory neurons and leads to reduction of multiple forms cortical plasticity [7,18,19,21,22]. All of these effects may have important implications for subsequent cortical function, cognition and behavior in human infants with preterm brain injury.

Acknowledgments

References

1. Blencowe H, Cousens S, Oestergaard MZ, Chou D, Moller A-B, Narwal R, et al. National, regional, and worldwide estimates of preterm birth rates in the year 2010 with time trends since 1990 for selected countries: a systematic analysis and implications. The Lancet. 2012 Jun 15.379:2162–2172.

2. The Lancet. The global burden of preterm birth. The Lancet. 2009 Oct.374:1214.

3. Moore T, Hennessy EM, Myles J, Johnson SJ, Draper ES, Costeloe KL, et al. Neurological and developmental outcome in extremely preterm children born in England in 1995 and 2006: the EPICure studies. BMJ. 2012; 345doi: 10.1136/bmj.e7961

4. Volpe, JJ. Neurology of the newborn. 5. Philadelphia: Saunders/Elsevier; 2008. Available from: http://www.loc.gov/catdir/toc/ecip083/2007044207.html

5. Ferriero DM. Neonatal Brain Injury. N Engl J Med. 2004; 351:1985–1995. [PubMed: 15525724]

6. McQuillen PS, Sheldon RA, Shatz CJ, Ferriero DM. Selective vulnerability of subplate neurons after early neonatal hypoxia-ischemia. J Neurosci. 2003 Apr 15.23:3308–15. [PubMed: 12716938]

7. Failor S, Nguyen V, Darcy DP, Cang J, Wendland MF, Stryker MP, et al. Neonatal cerebral hypoxia-ischemia impairs plasticity in rat visual cortex. J Neurosci. 2010 Jan 6.30:81–92. [PubMed: 20053890]

8. Back SA, Han BH, Luo NL, Chricton CA, Xanthoudakis S, Tam J, et al. Selective vulnerability of late oligodendrocyte progenitors to hypoxia- ischemia. J Neurosci. 2002; 22:455–63. [PubMed: 11784790]

9. Sen E, Levison SW. Astrocytes and developmental white matter disorders. Ment Retard Dev Disabil Res Rev. 2006; 12:97–104. [PubMed: 16807889]

10. Hagberg H, Mallard C, Ferriero DM, Vannucci SJ, Levison SW, Vexler ZS, et al. The role of inflammation in perinatal brain injury. Nat Rev Neurol. 2015 Apr.11:192–208. [PubMed: 25686754]

11. Allendoerfer KL, Shatz CJ. The subplate, a transient neocortical structure: its role in the development of connections between thalamus and cortex. Annu Rev Neurosci. 1994; 17:185–218. [PubMed: 8210173]

12. Kanold PO, Luhmann HJ. The subplate and early cortical circuits. Annu Rev Neurosci. 2010; 33:23–48. [PubMed: 20201645]

13. Luhmann HJ, Kilb W, Hanganu-Opatz IL. Subplate cells: amplifiers of neuronal activity in the developing cerebral cortex. Front Neuroanat. 2009; 3:19. [PubMed: 19862346]

14. McConnell SK, Ghosh A, Shatz CJ. Subplate neurons pioneer the first axon pathway from the cerebral cortex. Science. 1989 Sep 1.245:978–82. [PubMed: 2475909]

15. Friauf E, McConnell SK, Shatz CJ. Functional synaptic circuits in the subplate during fetal and early postnatal development of cat visual cortex. J Neurosci. 1990 Aug.10:2601–13. [PubMed: 2388080]

16. Friauf E, Shatz CJ. Changing patterns of synaptic input to subplate and cortical plate during development of visual cortex. J Neurophysiol. 1991 Dec.66:2059–71. [PubMed: 1812236]

17. Finney EM, Stone JR, Shatz CJ. Major glutamatergic projection from subplate into visual cortex during development. J Comp Neurol. 1998 Aug 17.398:105–18. [PubMed: 9703030]

18. Kanold PO, Kara P, Reid RC, Shatz CJ. Role of subplate neurons in functional maturation of visual cortical columns. Science. 2003 Jul 25.301:521–5. [PubMed: 12881571]

19. Kanold PO, Shatz CJ. Subplate neurons regulate maturation of cortical inhibition and outcome of ocular dominance plasticity. Neuron. 2006 Sep 7.51:627–38. [PubMed: 16950160]

20. Dupont E, Hanganu IL, Kilb W, Hirsch S, Luhmann HJ. Rapid developmental switch in the mechanisms driving early cortical columnar networks. Nature. 2006 Jan 5.439:79–83. [PubMed: 16327778]

21. Tolner EA, Sheikh A, Yukin AY, Kaila K, Kanold PO. Subplate neurons promote spindle bursts and thalamocortical patterning in the neonatal rat somatosensory cortex. J Neurosci. 2012 Jan 11.32:692–702. [PubMed: 22238105]

22. Ranasinghe S, Or G, Wang EY, Ievins A, McLean MA, Niell CM, et al. Reduced Cortical Activity Impairs Development and Plasticity after Neonatal Hypoxia Ischemia. J Neurosci Off J Soc Neurosci. 2015 Aug 26.35:11946–11959.

23. Bayer SA, Altman J. Development of layer I and the subplate in the rat neocortex. Exp Neurol. 1990; 107:48–62. [PubMed: 2295319]

24. Lein ES, Hawrylycz MJ, Ao N, Ayres M, Bensinger A, Bernard A, et al. Genome-wide atlas of gene expression in the adult mouse brain. Nature. 2007 Jan 11.445:168–176. [PubMed: 17151600]

25. Hoerder-Suabedissen A, Molnar Z. Molecular Diversity of Early-Born Subplate Neurons. Cereb Cortex. 2012 May 23.23:1473–1483. [PubMed: 22628460]

26. West MJ, Slomianka L, Gundersen HJ. Unbiased stereological estimation of the total number of neurons in thesubdivisions of the rat hippocampus using the optical fractionator. Anat Rec. 1991 Dec.231:482–497. [PubMed: 1793176]

27. Hulley, SB.Cummings, SR.Browner, WS.Newman, TB., Hearst, N., editors. Designing clinical research: an epidemiologic approach. Baltimore: Williams & Wilkins; 1988.

28. West MJ. Optimizing the sampling scheme for a stereological study: how many individuals, sections, and probes should be used. Cold Spring Harb Protoc. 2013 Jun.2013:521–532. [PubMed: 23734015]

29. Okusa C, Oeschger F, Ginet V, Wang W-Z, Hoerder-Suabedissen A, Matsuyama T, et al. Subplate in a rat model of preterm hypoxia-ischemia. Ann Clin Transl Neurol. 2014 Sep.1:679–691. [PubMed: 25493282]

30. Rice, JEd, Vannucci, RC., Brierley, JB. The influence of immaturity on hypoxic-ischemic brain damage in the rat. Ann Neurol. 1981; 9:131–41. [PubMed: 7235629]

31. Towfighi J, Mauger D, Vannucci RC, Vannucci SJ. Influence of age on the cerebral lesions in an immature rat model of cerebral hypoxia-ischemia: a light microscopic study. Brain Res Dev Brain Res. 1997; 100:149–60. [PubMed: 9205806]

32. Sizonenko SV, Sirimanne E, Mayall Y, Gluckman PD, Inder T, Williams C. Selective cortical alteration after hypoxic-ischemic injury in the very immature rat brain. Pediatr Res. 2003 Aug. 54:263–9. [PubMed: 12736386]

33. Sizonenko SV, Kiss JZ, Inder T, Gluckman PD, Williams CE. Distinctive Neuropathologic Alterations in the Deep Layers of the Parietal Cortex after Moderate Ischemic-Hypoxic Injury in the P3 Immature Rat Brain. Pediatr Res. 2005 Jun.57:865–872. [PubMed: 15774844]

34. Brockmann MD, Kukovic M, Schönfeld M, Sedlacik J, Hanganu-Opatz IL. Hypoxia-Ischemia Disrupts Directed Interactions within Neonatal Prefrontal-Hippocampal Networks. PLoS ONE. 2013 Dec 20.8:e83074. [PubMed: 24376636]

35. Sheldon RA, Sedik C, Ferriero DM. Strain-related brain injury in neonatal mice subjected to hypoxia-ischemia. Brain Res. 1998; 810:114–22. [PubMed: 9813271]

36. Sizonenko SV, Camm EJ, Garbow JR, Maier SE, Inder TE, Williams CE, et al. Developmental changes and injury induced disruption of the radial organization of the cortex in the immature rat brain revealed by in vivo diffusion tensor MRI. Cereb Cortex. 2007 Nov.17:2609–17. [PubMed: 17259644]

37. Segovia KN, McClure M, Moravec M, Luo NL, Wan Y, Gong X, et al. Arrested oligodendrocyte lineage maturation in chronic perinatal white matter injury. Ann Neurol. 2008 Apr.63:520–30. [PubMed: 18393269]

38. Robertson RT, Annis CM, Baratta J, Haraldson S, Ingeman J, Kageyama GH, et al. Do subplate neurons comprise a transient population of cells in developing neocortex of rats? J Comp Neurol. 2000; 426:632–650. [cited 2013 Jul 26]. [PubMed: 11027404]

39. McQuillen PS, DeFreitas MF, Zada G, Shatz CJ. A novel role for p75NTR in subplate growth cone complexity and visual thalamocortical innervation. J Neurosci. 2002 May 1.22:3580–93. [PubMed: 11978834]

40. Ferland RJ, Cherry TJ, Preware PO, Morrisey EE, Walsh CA. Characterization of Foxp2 and Foxp1 mRNA and protein in the developing and mature brain. J Comp Neurol. 2003 May 26.460:266–279. [PubMed: 12687690]

41. Hisaoka T, Nakamura Y, Senba E, Morikawa Y. The forkhead transcription factors, Foxp1 and Foxp2, identify different subpopulations of projection neurons in the mouse cerebral cortex. Neuroscience. 2010 Mar 17.166:551–563. [PubMed: 20040367]

42. Nguyen V, McQuillen PS. AMPA and metabotropic excitoxicity explain subplate neuron vulnerability. Neurobiol Dis. 2010 Jan.37:195–207. [PubMed: 19822212]

43. Chun JJ, Shatz CJ. The earliest-generated neurons of the cat cerebral cortex: characterization by MAP2 and neurotransmitter immunohistochemistry during fetal life. J Neurosci. 1989 May. 9:1648–67. [PubMed: 2566660]

44. Kanold PO. Transient microcircuits formed by subplate neurons and their role in functional development of thalamocortical connections. Neuroreport. 2004 Oct 5.15:2149–53. [PubMed: 15371723]

45. Olavarria J, Van Sluyters RC. Organization and postnatal development of callosal connections in the visual cortex of the rat. J Comp Neurol. 1985 Sep 1.239:1–26. [PubMed: 4044927]

46. Viswanathan S, Bandyopadhyay S, Kao JP, Kanold PO. Changing microcircuits in the subplate of the developing cortex. J Neurosci. 2012 Feb 1.32:1589–601. [PubMed: 22302801]
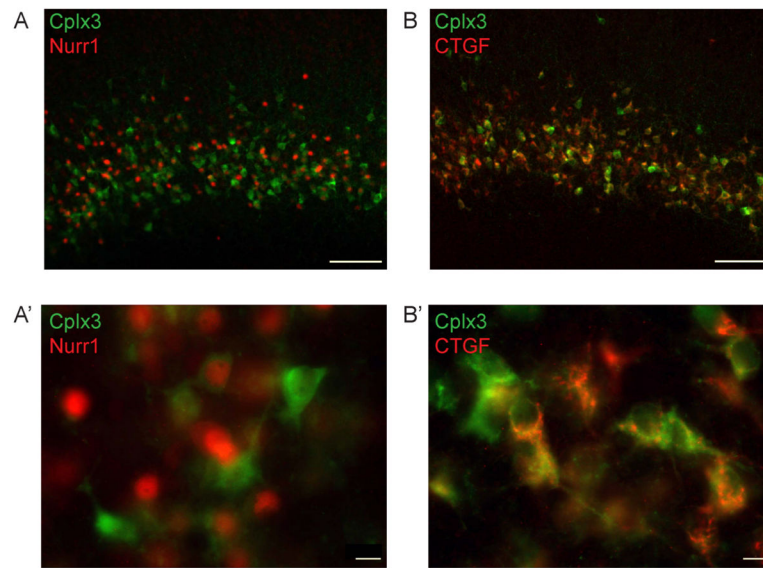
Figure 1. Subplate markers Nurr1 and CTGF colabel some cells with Cplx3

P8 rat control brain stained with subplate markers Complexin3 (green) and Nurr1 (red) (panel A) or Complexin3 (green) and CTGF (red) (panel B) show cells positive for both or either markers. Scale bar: 100um. Corresponding panels (A′ and B′) show a close up of single positive and double positive cells. Scale bar: 10 um.
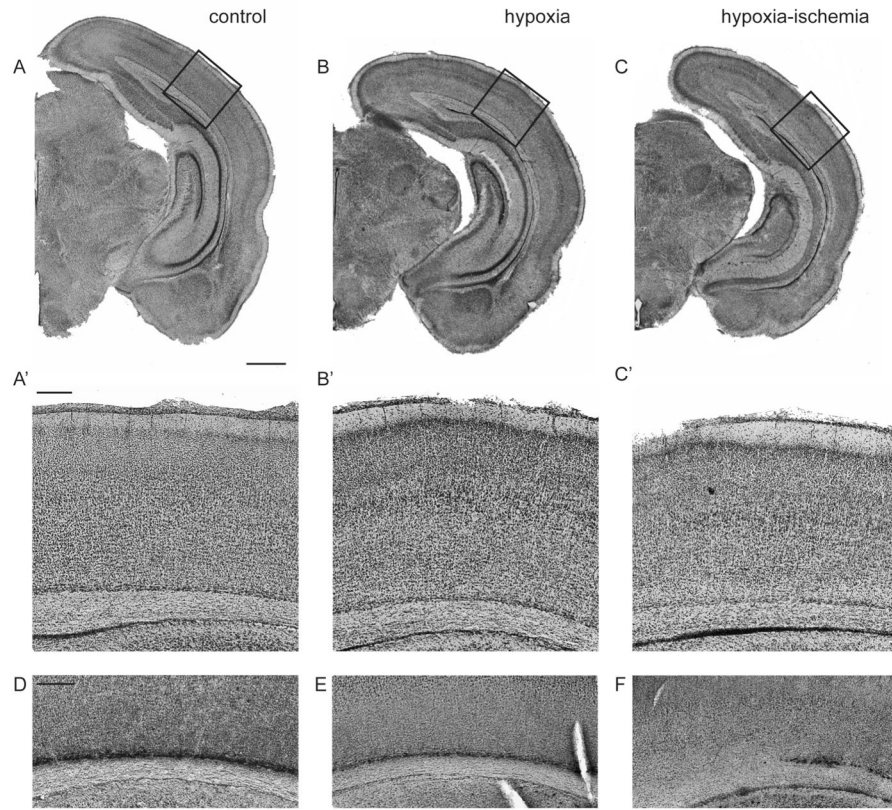
Figure 2. Histological assessment of moderate cortical injury following hypoxia ischemia in P8 rat

Cresyl violet stained coronal sections of the three examined conditions: naive control (A), hypoxia (contralateral to injury, B), hypoxia-ischemia (ipsilateral to injury, C). Scale bar: 1mm. Corresponding panels (A′, B′, C′) show a close up of the areas indicated by black boxes. Comparable regions stained for Complexin3 with DAB show normal subplate (D), thinning subplate in hypoxia (E), and patches of subplate cell loss in HI (F). Scale bar: 200um for A′–F.
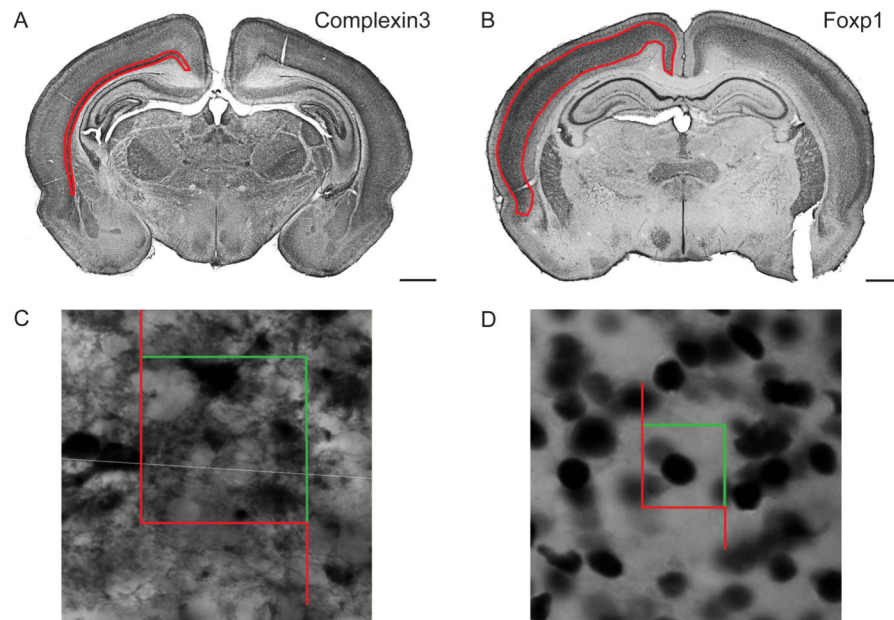
Figure 3. Regions of interest and counting frames for stereological quantification in P8 rat
DAB staining with subplate marker, Complexin3, (A) and layer III–V maker, Foxp1, (B). Contours in red indicate regions of interest used for analysis. Scale bar: 1mm. Example of a Complexin3+ cell (C, counting frame: 40umx40um) and Foxp1+ cell (D, counting frame: 20umx20um) counted using the Optical Fractionator probe.
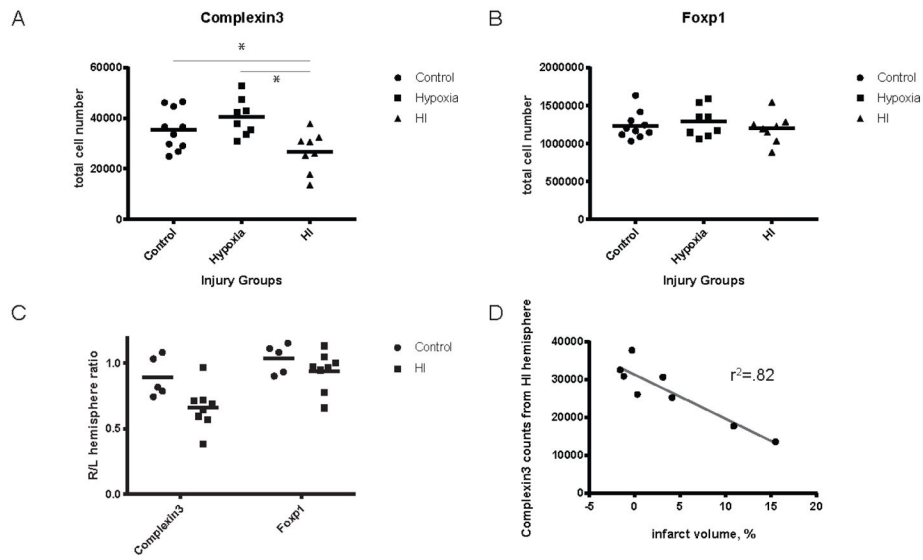
Figure 4. Quantification of Complexin3 and Foxp1 across injury groups at P8
Complexin3+ subplate population in HI group is significantly decreased compared to control and hypoxia group (A, p =0.0177 and p= 0.0015). Foxp1+ cell numbers are not significantly different between injury groups (B). Hemispheric (right/left) ratios of Complexin3 and Foxp1 counts show a greater variability in the injured groups, compared to controls (C). Complexin3 cell counts in HI hemisphere are negatively correlated with infarct volume as defined by (infarct volume = (hypoxia - hypoxia-ischemia)/hypoxia) (D, r^2=0.82, p=0.0017).
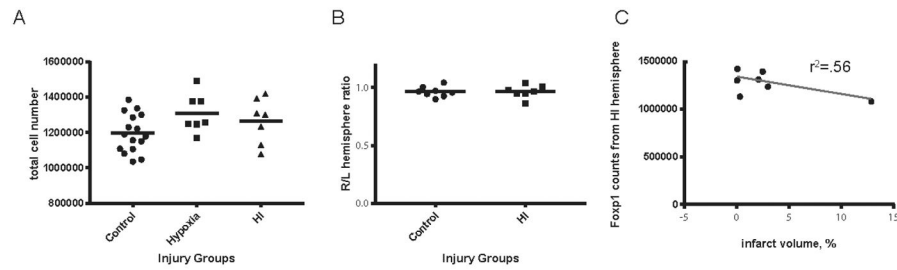
Figure 5. Quantification of Foxp1 across injury groups at P21

Foxp1+ cell numbers are not significantly different between injury groups (A). Hemispheric ratios (right/left) of Foxp1 counts have low variability between control and hypoxia (B). Foxp1 cell counts in HI hemisphere are not significantly correlated with infarct volume as defined by (infarct volume = (hypoxia - hypoxia-ischemia)/hypoxia) (C, r^2=0.56, p=0.1418).

Table 1

Stereology Study Parameters

Parameters reported for the stereology analysis of Complexin3 (at P8) and Foxp1 (at P8 and P21). Same counting parameters were used for control and injured hemispheres; estimates are reported for control and in parentheses HI. Estimated population (number weighted section thickness) is reported for mean N.

Parameters	P8, Cplx3	P8, Foxp1	P21, Foxp1
observed group mean, *Mean N*	35457 (26747)	1234640 (1195085)	1195632 (1265190)
observed coefficient of variation of group mean, *OCV*	0.23 (0.30)	0.14 (0.37)	0.023 (0.038)
number of individuals in group, *n*	5 (8)	5 (8)	8 (7)
observed coefficient of variation of estimator, *CE*	0.08 (0.10)	0.08 (0.08)	0.05 (0.05)
section sampling fraction, *ssf*	1/12	1/12	1/12
fraction of area of section sampled, *asf*	0.1024	0.0028	0.0064
thickness sampling fraction (h/t), *tsf*	0.61	0.66	0.57
disector volume, $h \times A_{frame}$	16000	4000	16000
average number of objects counted in each individual, ΣQ^-	208	204	366
thickness of mounted section, *t*	16.3μm	15μm	17.4 μm
height of disector, *h*	10 μm	10 μm	10 μm
guard zone	1μm	1μm	1μm
smoothness factor, *m*	1	1	1
number of sections used, *i*	5	5	8
counting frame, A_{frame}	40×40 μm^2	20×20 μm^2	40×40 μm^2
sampling grid area, A_{grid}	125×125 μm^2	375×375 μm^2	500×500 μm^2

[*] for the first 4 rows, numbers are reported as: control hemisphere (HI injured hemisphere)